

This is the author's final, peer-reviewed manuscript as accepted for publication. The publisher-formatted version may be available through the publisher's web site or your institution's library.

Thermochemical pretreatments for agricultural residue ash production for concrete

Feraidon F. Ataie and Kyle A. Riding

How to cite this manuscript

If you make reference to this version of the manuscript, use the following information:

Ataie, F. F., & Riding, K. A. (2013). Thermochemical pretreatments for agricultural residue ash production for concrete. Retrieved from <http://krex.ksu.edu>

Published Version Information

Citation: Ataie, F. F., & Riding, K. A. (2013). Thermochemical pretreatments for agricultural residue ash production for concrete. *Journal of Materials in Civil Engineering*, 25(11), 1703-1711.

Copyright: © 2013 American Society of Civil Engineers

Digital Object Identifier (DOI): doi:10.1061/(ASCE)MT.1943-5533.0000721

Publisher's Link: <http://ascelibrary.org/doi/abs/10.1061/%28ASCE%29MT.1943-5533.0000721>

This item was retrieved from the K-State Research Exchange (K-REx), the institutional repository of Kansas State University. K-REx is available at <http://krex.ksu.edu>

Thermochemical Pretreatments for Agricultural Residue Ash Production for Concrete

Feraidon F. Ataie¹ and Kyle A. Riding¹

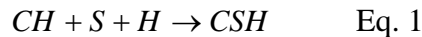
Abstract:

Agricultural residue ash is known to be a very reactive source of supplementary cementitious material (SCM) for use in concrete. The influence of thermochemical pretreatments on the reactivity of agricultural residue ash (ARA) for use as an SCM was studied. It was shown that pretreatments are effective in partial removal of alkali metals and other impurities out of both wheat straw and rice straw leading to ARA with lower loss on ignition (LOI), higher internal surface area, and higher amorphous silica content than that of untreated ARA. It was shown that the ash alkali content correlated with the ash LOI and amorphous silica content. When used at a cement replacement rate of 20% by mass, pretreated ARA accelerated the hydration of cement paste samples while untreated ARA retarded the cement hydration. Pretreatments were found to increase ARA reactivity as measured by calcium hydroxide content reduction with time. ARA increased compressive strength of mortar samples by 25% when used as 20% replacement of cement in the samples. It was found that the calcium hydroxide content of paste samples and mortar compressive strength were correlated to the amorphous silica content of the ash.

¹Dept. of Civil Engineering, Kansas State University, Manhattan, KS 66506

20 **Introduction:**

21 The use of supplementary cementitious material (SCM) can reduce the energy and CO₂
22 intensity of concrete. Natural SCMs have received increasing interest because of their high
23 reactivity, low cost, and availability in some regions where other SCMs are not available.
24 Agricultural residue ash (ARA) such as rice husk ash (RHA) and sugarcane bagasse ash have
25 been championed as SCMs that can greatly enhance strength and durability of concrete (Salas, et
26 al. 2009; Feng, et al. 2004; Nair, et al. 2006; Cordeiro, et al. 2006; Agarwal 2006; Tuan, et al.
27 2011; Sales and Sofia 2010). Other agro-biomass such as wheat straw (WS) and rice straw (RS)
28 could be a potential source for SCMs with similar pozzolanic reactivity to RHA. The pozzolanic
29 reaction is the reaction between a siliceous material and calcium hydroxide (CH) under water to
30 form a cementitious material, as shown in Eq. 1(Wanson, et al. 2009).



31 Note: Oxide notation is used throughout this paper, C = CaO, S = SiO₂, H=H₂O, A = Al₂O₃,
32 F=Fe₂O₃.

33 The pozzolanic reaction kinetics is known to be affected by many factors such as ash
34 mineralogy, surface area, and carbon content of the pozzolanic materials (Feng, et al. 2004;
35 Wanson, et al. 2010).

36 Agro-biomass pretreatment processes can enhance ARA reactivity for use in concrete.
37 Thermochemical pretreatment techniques, such as dilute acid, have been shown to improve
38 pozzolanic reactivity by increasing surface area and amorphous silica content and decreasing
39 carbon content of RHA (Feng, et al. 2004; Wanson, et al. 2009; Chandrasekhar, et al. 2006). In
40 the biofuel industry, thermochemical pretreatment of lignocellulosic biomass has proven to be
41 very effective hydrolysis process for ethanol production (Zheng, et al. 2009; Saha, et al. 2005;
42 Kristensen, et al. 2008; Mosier, et al. 2005). The dilute acid pretreatments are effective in

43 removal of some hemicellulose; breakdown, re-localization, and structure change of lignin; and
44 defibrillation/decrystallization of cellulose of the biomass cell wall. Pretreatment of agro-biomass
45 has been shown to improve combustion properties of biomass for use as a fuel as a result of
46 leaching impurities such as Na, K, Ca, and Mg (Jenkins, et al. 2003). These metals decrease the
47 biomass melting temperature and promote the release of unwanted byproducts during
48 combustion (Jenkins, et al. 2003).

49 The pozzolanic properties of rice straw ash (RSA) and wheat straw ash (WSA) have been
50 examined by only a few researchers. WSA that has not been pretreated has been found to be
51 pozzolanically reactive when burned at 570 °C and 670 °C for 5 hours (Biricik et al. 1999). Al-
52 Akhras and Abu-Alfoul (2002) have reported that mechanical properties of autoclaved mortar
53 specimens were improved with by WSA made by burning wheat straw at 650 °C for 20 hrs. RSA
54 has been shown to improve mechanical properties of mortar and concrete specimens through a
55 pozzolanic reaction (Francisco et al. 2008). One study showed that rice straw pretreated with
56 hydrolysis could produce good quality ash for use in concrete, however no comparison with
57 unpretreated rice straw ash was made to quantify the benefits of pretreatment (El-Damatty and
58 Hussain 2007). The impact of thermochemical pretreatments on the RSA and WSA sensitivity to
59 burning conditions and subsequent reactivity in a cementitious system has not been studied.
60 Additionally, the mechanism by which pretreatments improve ARA pozzolanicity has not been
61 fully established.

62 This paper documents the effects of thermochemical pretreatments on the physical properties,
63 chemical properties, and reactivity of WSA and RSA in a cementitious system. Employing
64 several pretreatments techniques and burning conditions, this study attempts to examines the
65 mechanism(s) by which pretreatments enhance ARA reactivity. Distilled water (DW) and 0.1 N

66 hydrochloric acid (HCl) were used to pretreat the biomass at 23°C, 50°C and 80°C for several
67 soaking durations followed by burning at 500°C, 650°C, 700°C, and 800°C. Loss on ignition
68 (LOI), internal surface area, and amorphous silica content of ARA were measured for these
69 ashes. Isothermal calorimetry, thermogravimetric analysis, electrical conductivity measurements,
70 and mortar compressive strength were used to quantify the ARA reactivity.

71 **Materials:**

72 An ASTM C 150 (2009) Type I/II portland cement was used for this study with the
73 cement properties shown in Table 1. Standard graded sand (ASTM 2006) was used for the
74 mortar experiments. Wheat straw (WS) was purchased from Britt's farm in Manhattan, KS and
75 Rice straw (RS) was obtained from Missouri Rice Research Farm, Glennonville, Missouri.
76 Reagent grade HCl was obtained and diluted to 0.1 N for use in the study.

77 **Experimental methods:**

78 Hydrothermal and thermochemical pretreatment methods were performed on the WS and RS
79 using distilled water (DW) and 0.1 N HCl. To pretreat the biomass, 250 g of biomass was
80 immersed in 3100±100 mL of the solution in a 4000 mL glass jar. The sample was stored
81 undisturbed at a constant temperature for the immersion period of interest. Three different
82 temperatures, 23°C, 50°C, and 80°C, were used to make ash for each pretreatment method which
83 will be referred to as DW23°C, DW50°C, and DW80°C for the distilled water pretreatment at
84 23°C, 50°C, and 80°C and HCl23°C, HCl50°C, and HCl80°C for the 0.1 N HCl pretreatment at
85 23°C, 50°C, and 80°C, respectively. AR samples were immersed for 0.5, 1, 2, 4, 8, and 24 hrs
86 before burning. Leachate samples were collected from two separate containers of pretreated AR
87 for each time and temperature. The Mg, Ca, K, and Na concentration was measured using
88 atomic absorption spectroscopy (AAS) for each container. The Mg, Ca, K, and Na concentration

89 was reported as the average concentration of the two containers. After pretreatment, the biomass
90 was rinsed twice with distilled water and dried at 80°C for storage until burning. 200 g of
91 biomass was burned in each ARA batch made. A stainless steel cage with two wire mesh
92 shelves was used to hold the biomass during burning. A stainless steel pan was placed below the
93 cage to catch any ash that fell through the mesh. A programmable electric muffle furnace was
94 used to heat the samples to a predetermined temperature and hold time. Samples were heated to
95 500°C, 650°C, 700°C, or 800°C using 1, 2, or 3 hr soak times. Finally, the ash was ground for
96 one hour at 85 revolutions per minute (rpm) in a laboratory ball mill.

97 Particle-size distribution and internal surface area of the ground ARA were determined using
98 a laser diffractometer and BET nitrogen adsorption respectively. LOI of ARA was determined by
99 measuring the mass loss after heating one gram of dry ARA (WSA or RSA) to 800°C for 3 hrs.
100 LOI was calculated as the percentage mass loss during firing.

101 To measure the amorphous silica content of ARA, the ash impurities and soluble material
102 content were measured (Nair, et al. 2006). The impurities content was measured by first boiling
103 0.5 g of ARA after the LOI test in 25 mL of 10% nitric acid. After boiling in acid the sample was
104 filtered through a glass microfiber filter paper with 1.1 µm openings and rinsed with deionized
105 water. The sample was then dried at 90±10°C and weighed. To measure the ash soluble material
106 content, 3 g of ARA was boiled in 200 mL of 10% sodium hydroxide solution (2.5 N NaOH) for
107 5 minutes. After boiling, the sample was cooled to room temperature, filtered through a 1.1 µm
108 glass microfiber filter paper, and washed with deionized water. The residue and filter paper was
109 then heated to 800 °C for 3 hrs. The ash weight change after boiling in the sodium hydroxide and
110 heating was recorded. The ARA amorphous silica content was then calculated using Eq. 2 :

$$Si_{am} = w_{sol} - LOI - w_{im} \quad \text{Eq. 2}$$

111 where Si_{am} is the amorphous silica content of the ash (%), w_{sol} is the ash weight loss after boiling
112 in sodium hydroxide and heating (%), LOI is the ash loss on ignition (%), and w_{im} is the weight
113 of impurities (%).

114 The decrease in electrical conductivity of a calcium hydroxide solution mixed with SCMs
115 has been used by other researchers as a simple reactivity index for pozzolanic behavior of SCMs
116 (Sinthaworn and Nimityongskul 2009; Paya, et al. 2001) and was used in this study. One gram
117 of ARA was mixed with 100 mL of saturated calcium hydroxide solution at 23 ± 2 °C. The
118 solution's electrical conductivity was then measured for 7 days.

119 For the cement paste experiments, ARA was used at a 20% replacement level by mass of
120 cement when used. A water-cementitious materials ratio (w/cm) of 0.5 was used for all paste
121 samples. The paste samples were mixed using a procedure previously used (Riding, et al. 2010).
122 Distilled water was added to the cementitious material and mixed using a vertical laboratory
123 mixer at 500 rpm for 90 seconds, followed by a 120 second rest period, and finally mixed at
124 2000 rpm for 120 seconds.

125 Isothermal calorimetry was used to study the reaction rate of ARA in a cementitious system.
126 An eight-channel isothermal calorimeter was used in this study at 23°C. Paste samples of
127 approximately 30 g each were used. The calcium hydroxide (CH) content of cement paste
128 samples was measured by thermogravimetric analysis to study the pozzolanic consumption of
129 CH by ARA. Samples were wet cured starting at 24 hrs after casting at 23 °C. Cement paste
130 hydration was stopped at 7, 28, and 90 days after mixing by means of solvent exchange with
131 isopropanol. 3-5mm thick samples were cut and placed in isopropanol for 7 days. After 7 days
132 in isopropanol, the samples were dried in a vacuum for at least 3 days. For thermogrametric
133 analysis, samples were heated at 20°C/min up to 900 °C in a nitrogen environment.

134 Mortar cube compressive strength was measured according to ASTM C 109 (2008) with a
135 sand to cementitious material ratio of 2.75. A w/cm of 0.55 was used for all mortar samples
136 because of the decreased workability of systems with ARA. ARA was used at a 20%
137 replacement level by mass of cement when used. Mortar cube compressive strength was tested at
138 7 and 28 days with the results reported as the average of the compressive strength of three mortar
139 cubes.

140 **Results and discussion:**

141 **Pretreatments and alkali leaching**

142 Pretreatments were very effective in altering the chemical and physical structure of the
143 straw and removing K, Ca, and Mg. Figure 1 shows the leachate K concentrations for different
144 pretreatments used for WS. The sodium concentrations were found to be much lower than K, and
145 varied only slightly by pretreatment method. Figure 2 shows the calcium (Ca) and magnesium
146 (Mg) leachate concentration for WS. HCl and higher temperatures increased the leaching rates of
147 K, Ca, and Mg. A much larger difference between HCl and DW pretreatments was seen
148 however with Ca and Mg removal from WS than K and Na. Similar trends were observed for
149 RS. The temperature sensitivity of K removal during pretreatments was quantified by calculating
150 the dissolution activation energy. First, the leachate K concentration with time for a given
151 pretreatment temperature was fit to
152 Eq. 3 (ASTM, 2010):

$$153 \quad C(t) = C_{ult} \frac{K \cdot (t)}{1 + K \cdot (t)} \quad \text{Eq. 3}$$

154 where $C(t)$ is the potassium concentration as a function of soaking duration (ppm), t is the time
155 passed after starting the pretreatment (days), C_{ult} is the ultimate potassium concentration assumed

156 to be equal to the concentration measured at 24 hr of treatment (ppm), and K is the rate constant
157 of potassium dissolution. The Arrhenius plot was made by plotting the natural log of the rate
158 constant K against the reciprocal of the pretreatment temperature in Kelvins. Figure 3 shows the
159 Arrhenius plot for the rate constants calculated for the leachate K concentration for wheat straw.
160 The activation energy was calculated as the slope of the fit line on the Arrhenius plot multiplied
161 by the universal gas constant R (8.314 J/mol/K). The activation energy for leaching K with 0.1
162 N HCl was found to be 32.2 KJ/mol, versus 13.3 KJ/mol with DW pretreatments. This shows
163 that the higher the acid concentration the more effectively heat can be used to remove K from the
164 AR with high acid concentrations.

165 **Surface area, LOI and amorphous silica content of ARA**

166 Pretreatments were effective in reducing the carbon content in the ARA, increasing the
167 internal surface area, and increasing the percentage of amorphous silica in the ash. Figure 4
168 shows the amorphous silica content of ARA. For a given burning temperature, pretreatments
169 increased the amorphous silica content. Pretreated ARA burned at 500°C for 2 hrs had a similar
170 amorphous silica content as the one burned at 650°C for 1 hr. The untreated WSA had 21%
171 crystalline silica and untreated RSA had 19% crystalline silica when burned at 650°C for 1
172 hour as calculated from the ash total silica content shown in Table 2 and the ash amorphous
173 silica content shown in Figure 4. The ash pretreated with 0.1N HCl at 80°C showed little if any
174 crystalline silica while the WSA pretreated with DW at 80°C had 8% crystalline silica. The
175 increase in amorphous silica content of the pretreated ARA correlated with the removal of Ca,
176 Mg, and K out of the biomass by pretreatments. Figure 5 shows the amorphous silica content of
177 ARA versus the CaO, MgO, and K₂O content. The amorphous silica content of the ARA
178 corresponded with a decrease in the CaO, MgO, and K₂O content, with the MgO showing a

179 slightly better correlation. Figure 6 shows the LOI measured for WSA and RSA. The ARA LOI
180 decreases as the burning temperature increases regardless of the pretreatment type. At a given
181 burning temperature, pretreated ARA had a lower LOI than that of the untreated control ash.
182 Figure 7 shows the metal impurity (Ca, Mg, and K) content of the ash for the WSA and RSA was
183 also correlated to the ARA LOI. The RSA had a lower LOI than the corresponding WSA,
184 possibly because of the lower alkali content of the RSA before pretreatment than the WSA. Even
185 though distilled water pretreatments were not as effective as the more acidic pretreatments, when
186 burned at 650°C for 1hr the WSA pretreated with DW23/24 still had 52% lower LOI and 15%
187 higher amorphous silica than that of untreated WSA. RSA pretreated with DW23/24 had 55%
188 lower LOI and 17% higher amorphous silica than that of untreated RSA.

189 Another important impact of the pretreatments is the decrease in temperature sensitivity of
190 the biomass. Sensitivity reduction is vital for low cost ARA production in using simple kilns or
191 large scale applications where it may be more difficult to control the temperature. The
192 pretreatments were very effective in reducing the sensitivity to burning temperatures. The
193 HCl80/24 WSA burned at 800 °C had a higher amorphous SiO₂ content than that of the control
194 burned at 500°C as shown in Figure 4.

195 LOI and amorphous silica content of ARA was shown to be affected by the duration of
196 burning. Table 4 shows the LOI and amorphous silica content for WSA pretreated with 0.1N
197 HCl at 80°C for 24 hours and then burned at different temperatures and holding durations. There
198 appears to be an optimum burning time for each temperature which appeared to coincide with the
199 removal of most of the carbon. At 500°C, the optimum burning time was found to be between
200 one and two hours whereas at 600°C it was found to be less than or equal to one hour. Burning

201 periods longer than the optimum time did not appear to improve amorphous silica content or
202 LOI.

203 The pretreatment changed the color of the ash, mainly because of the decrease in carbon
204 content. Figure 8A shows WSA pretreated with 0.1N HCl at 80°C for 24 hrs, while Figure 8B
205 shows control WSA samples ashed at four different temperatures. The WSA-HCL80/24 ash was
206 much lighter in color than that of control WSA ashes regardless of the burning condition. Even
207 though it had a low LOI, the WSA pretreated with HCl at 80°C for 24 hrs and burned at 800°C
208 for one hr had a slightly darker color than the pretreated ashes made at lower temperatures
209 (Figure 8A). Although the color of the ash is largely related to carbon content of the ash,
210 impurities such as alkali metals can change the ash color. At higher temperatures these metals
211 react with silicon (Si) to produce crystalline phases that may combined with carbon or contain
212 iron giving the ash a darker color (Muthadhi and Kothandaraman 2010; Genieva, et al. 2011). It
213 was also observed that washing the biomass after pretreatments is very important in removing
214 alkalis from surface of biomass and reducing LOI of the resulted ash. This could be because
215 when the straw was not washed after the pretreatment, potassium and other impurities in solution
216 would precipitate on to the surface of the straw during drying. These precipitates could trap
217 carbon during ashing, leading to higher ash LOI. Even though pretreatments remove metal
218 impurities out of the biomass cell wall, it is beneficial to wash the biomass after pretreatment to
219 limit the impurities that would precipitate on the biomass surface. For a given burning condition,
220 pretreated but unwashed biomass resulted in ARA with darker color and higher LOI compared to
221 the ash obtained from pretreated and washed biomass. This could be attributed alkalis on the
222 surface melting at lower temperature and trapping carbon.

223 Table 3 presents the ARA surface area determined by BET nitrogen adsorption while Figure
224 9 shows the particle-size distribution for some selected ARAs. For a given pretreatment, ashes
225 burned at 500°C for 2 hrs had higher surface area than those burned at higher temperatures. This
226 is probably because at higher temperatures melting of some material may occur eliminating
227 pores inside of the ash. The particle-size distribution was not significantly affected by
228 pretreatments. Although the surface area of unpretreated RSA and WSA were similar, pretreated
229 RSA had a larger surface area than that of pretreated WSA.

230 **Conductivity measurements**

231 Figure 10 shows the normalized conductivity (the measured conductivity divided by the
232 initial conductivity of the solution) data for WSA pretreated with 0.1N HCl at 23°C, 50°C, and
233 80°C and burned at 500°C for 2 hours and 650°C for 1 hour. The normalized conductivity for
234 unpretreated WSA and WSA pretreated with DW and 0.1 N HCl is given in Figure 11. The
235 pretreatment temperature did not significantly affect the measured conductivity change. WSA
236 burned at 500°C for 2 hrs shows a more rapid drop in conductivity than WSA burned at 650°C
237 for 1 hour indicating a higher reactivity consistent with the higher surface ash measured in the
238 samples burned at 500°C. Very little difference was seen between different pretreatments in the
239 conductivity experiments. Similar behavior was seen for RSA conductivity experiments. The
240 initial increase in the electrical conductivity from the control sample is likely the result of
241 dissolution of metal impurities such as Na, K, Ca, and Mg in the solution (Sinthaworn, et al.
242 2011).

243 **Isothermal Heat of Hydration**

244 Figure 12 compares the heat of hydration for WSA burned at 650°C for 1 hour with and
245 without thermochemical pretreatments. Large differences in hydration behavior were seen

246 between the pretreated and control WSA. Figure 13 shows the total heat of hydration of cement
247 paste samples containing WSA. The pretreated ashes show similar total heat of hydration during
248 the first 120 hours, indicating a similar degree of cement hydration at 120 hours. Figure 14
249 shows the heat flow rate for paste samples containing RSA. The hydration rate of pretreated
250 ARA was accelerated compared to the control samples, whereas the samples with ARA that were
251 not pretreated were retarded as seen in Figure 12 and Figure 14. The hydration acceleration is
252 most likely caused by increased nucleation because of the very high ARA surface area (Bullard,
253 et al. 2011; Scrivener and Nonat 2011). Also, the samples containing pretreated ARA (WSA and
254 RSA) showed much more similar behavior to each other during the first 120 hours after mixing
255 than the non-pretreated ARA.

256 **Pozzolanic Reactivity**

257 The decrease in CH content of cement paste samples containing ARA is a measure of the
258 ARA pozzolanic reaction. The CH content for cement paste samples with and without ARA was
259 measured using TGA at 7, 28, and 90 days of hydration as shown in Figure 15 and 16 for WSA
260 and RSA, respectively. For a given pretreatment type and age, samples containing ARA (WSA
261 or RSA) burned at 500°C for 2 hr had a lower CH content than those burned at higher
262 temperatures. This can be attributed to the higher surface area of ARA burned at 500°C for 2 hr.
263 At a given burning condition, samples containing ARA pretreated with 0.1N HCl at 80°C for 24
264 hrs had a lower CH content than any other pretreatment type. At a given age, samples containing
265 WSA at burned at 500°C showed lower CH content than those containing RSA burned at 500°C.

266 Figure 17 shows the compressive strength development for mortar with and without 20%
267 cement replaced by ARA. The WSA and RSA pretreated with HCl at 80°C for 24 hours showed
268 the highest compressive strength development, with a 25% increase in strength over the ordinary

269 portland cement (OPC) mixture at 28 days of age. The increased strength seen with pretreated
270 ashes confirms the increased pozzolanic reaction seen with the reduction of CH content with
271 time in samples containing the pretreated ARA.

272 A comparison of the ARA material characteristic improvement from the pretreatments
273 (amorphous silica and surface area) and CH content at 90 days is shown in Figure 18. The
274 increase in amorphous silica content of ARA and surface area correlated with a decrease in the
275 CH content of paste samples containing ARA and increases compressive strength of mortar
276 samples containing ARA. The isothermal calorimetry results did not show a reduced hydration
277 development with the use of ARA indicating that the decrease in CH content seen with the ARA
278 is likely from the pozzolanic reaction and not a lower cement degree of hydration. Additionally
279 the OPC mixture showed an increase in CH content while the mixtures with ARA showed a
280 decrease in CH between 7 and 28 days.

281 **Conclusions:**

282 The material physical and pozzolanic properties of wheat straw ash (WSA) and rice straw ash
283 (RSA) were studied. From this study, the following conclusions can be made:

284 1- Pretreatments are effective in partial removal of Ca, K, and Mg out of the biomass. The
285 activation energy for K leaching was higher for dilute acid pretreatment than distilled
286 water pretreatment. This shows that heating samples during pretreatment even more
287 effective for the more acidic pretreatments.

288 2- Pretreatments increased the amorphous silica content and surface area and decreased the
289 LOI of ARA at a given burning temperature. It was shown that amorphous silica content
290 inversely correlated with the Ca, K, and Mg content of the ash while LOI of ARA is
291 directly correlated with the Ca, K, and Mg content of the ash. Alkalis seemed to encase or

292 combine with carbon during burning. Pretreatments reduced the sensitivity of the ash to
293 the burning temperature, showing less of a decrease in amorphous silica content than the
294 non-pretreated ash at 700°C and 800°C.

295 3- Pretreatments improved the system hydration kinetics. Non-pretreated ARA retarded the
296 cement hydration, whereas pretreated WSA and RSA accelerated the cement hydration.
297 The acceleration may be from increased nucleation from the increased material surface
298 area.

299 4- Cement paste sample containing ARA burned at 500°C for 2 hrs contained lower CH
300 than those samples containing ARA burned at 650°C for 1 hr. This was attributed to the
301 higher surface area of the ash burned at 500°C for 2 hrs. It was shown that CH content of
302 the paste after 90 days of hydration was inversely correlated with amorphous silica
303 content and surface area of the ash used in the paste. Samples containing WSA showed
304 lower CH content at 90 days than the RSA with similar surface area and amorphous silica
305 content.

306 5- When used as 20% replacement of cement in mortar samples, pretreated ARA increased
307 compressive strength of mortar samples at 28 days by 25% compared to the OPC sample.
308 Mortar samples containing pretreated ARA showed a 32% increase in 28 day
309 compressive strength compared to samples containing unpretreated ARA. It was also
310 shown that mortar compressive strength correlated well with the ash amorphous silica
311 content.

312 **Acknowledgements:**

313 Financial support for this project was provided by the National Science Foundation (CMMI-
314 103093). The authors thank Dr. Donn Beighley for providing the rice straw. The help of Dr.

315 Kenneth J. Klabunde for providing access to the BET Nitrogen equipment is appreciated. The
316 help of Monarch Cement Company in chemical analysis of samples is greatly acknowledged.
317 Valuable advice from Dr. Maria Juenger throughout this paper is greatly appreciated. Antoine
318 Borden's assistance with the pretreatment experiments is gratefully acknowledged.

319

320 **References**

321 Agarwal, S.K. (2006) "Pozzolanic activity of various siliceous materials." *Cement and Concrete*
322 *Research*, 36(9), 1735-1739.

323 Al-Akhras, N.M., and B.A. Abu-Alfoul. (2002) "Effect of wheatstrawash on mechanical
324 properties of autoclaved mortar." *Cement and Concrete Research*, 32(6), 859-863.

325 ASTM. (2010) "Standard Practice for Estimating Concrete Strength by the Maturity Method."
326 *C1074*, West Conshohocken, PA.

327 ASTM. (2009) "Standard Specification for Portland Cement." *C150*, West Conshohocken, PA.

328 ASTM. (2006) "Standard Specification for Standard Sand." *C778*, West Conshohocken, PA.

329 ASTM. (2008) "Standard Test Method for Compressive Strength of Hydraulic Cement Mortars."
330 *C109*, West Conshohocken, PA.

331 Biricik, H., F. Akoz, I. Berkaty, and A.N. Tulgar. (1999) "Study of pozzolanic properties of
332 wheat straw ash." *Cement and Concrete Research*, 29(5), 637-643.

333 Bullard, J.W., H.M. Jennings, R.A. Livingston, A. Nonat, G.W. Scherer, G.W., J.|S. Schweitzer,
334 K.L. Scrivener, J.J. Thomas. (2011) "Mechanisms of cement hydration." *Cement and Concrete*
335 *Research*, 41(12), 1208-1223.

336 Chandrasekhar, S., P.N. Pramada, and J. Majeed. (2006) "Effect of calcination temperature and
337 heating rate on the optical properties and reactivity of rice husk ash." *Journal of Materials*
338 *Science*, 41(23), 7926-7933.

339 Cordeiro, G.C., R.D. Toledo-Filho, and E.M. Rego-Fairbairn. (2006) "Use of ultrafine rice husk
340 ash with high-carbon content as pozzolan in high performance concrete." *Materials and*
341 *Structures*, 42(7), 983-992.

342 El-Damatty, A.A., and I. Hussain. (2007) "An economical solution fo the environmental problem
343 resulting from disposal of rice straw." *ERTEP*. Ghana, Africa: Springer, 15-24.

344 Feng, Q., H. Yamamichi, M. Shoya, and S. Sugita. (2004) "Study on the pozzolanic properties of
345 rice husk ash by hydrochloric acid pretreatment." *Cement and Concrete Research*, 34(3), 521-
346 526.

347 Francisco, T., J. Paul, and R. AustriacoLilia. (2008) "Compressive strenght of concrete blended
348 with calcined rice straw ash." *The 3rd ACF International Conference*. Ho Chi Minh, Vietnam,
349 592-597.

350 Genieva, S.D., S.C. Turmanova, and L.T. Vlaev. (2011) "Utilization of rice husks and the
351 products of its thermal degradation as fillers in polymer composites." Edited by S. Kalia, B.S.
352 Kaith and I. Kau. Springer, 345-375.

353 Jenkins, B.M., J.D. Mannapperuma, and R.R. Bakker. (2003) "Biomass leachate treatment by
354 reverse osmosis." *Fuel Processing Technology*, 81(3), 223-246.

355 Kristensen, J.B., L.G. Thygesen, C. Felby, H. Jorgensen, and T. Elder. (2008) "Cell-wall
356 structural changes in wheat straw pretreated for bioethonal production." *Biotechnology for*
357 *Biofuels*, 1(5).

358 Mosier, N., Wyman, C., Dale, B., Elander, R., Lee, Y.Y., Holtzapple, M., and Ladisch, M.
359 (2005) "Features of promising technologies for pretreatment of lignocellulosic biomass."
360 *Bioresources Technology*, 96(6), 673-686.

361 Muthadhi, A., and S. Kothandaraman. (2010) "Optimum production condiction for reactive rice
362 husk ash." *Materials and Structures*, 43(9), 1303-1315.

363 Nair, G., S. Jagadish, and A. Fraaij. (2006) "Reactive pozzolanas from rice husk ash: An
364 alternative to cement for rural housing." *Cement and Concrete Research*, 36(6), 1062-1071.

365 Paya, J., M.V. Borrachero, J. Monzo, and E, Peris-Mora. (2001) "Enhanced conductivity
366 measurement techniques for evaluation of fly ash pozzolanic activity." *Cement and Concrete*
367 *Research*, 31(1), 41-49.

368 Riding, K., D.A. Silva, and K. Scrivener. (2010) "Early age strength of blend cement systems by
369 CaCl₂ and diethanol-isopropanolmine." *Cement and Concrete Research*, 40(6), 935-946.

370 Saha, B.C., L.B. Iten, M.A. Cotta, and Y.V. Wu. (2005) "Dilute acid pretreatment, enzymatic
371 saccharification and fermentation of wheat straw to ethanol." *Process Biochemistry*, 40(12),
372 3693-3700.

373 Salas, A., S. Delvastoa, R.M. Gutierrez, and D. Lange. (2009) "Comparison of two processes
374 for treating rice husk ash for use in high performance concrete." *Cement and Concrete research*,
375 39(9), 773-778.

376 Sales, A., and L. Sofia. (2010) "Use of Brazilian sugarcae bagasse ash in concrete as sand
377 replacement." *Waste Management*, 30(6), 1114–1122.

378 Scrivener, K.L., and A. Nonat. (2011) "Hydration of cementitious materials, present and future."
379 *Cement and Concrete Research*, 41(7), 651-665.

380 Sinthaworn, S., and P. Nimityongskul. (2011) "Effects of temperature and alkaline solution on
381 electrical conductivity measurements of pozzolanic activity." *Cement and Concrete Research*,
382 33(5), 622-627.

383 Sinthaworn, S., and P. Nimityongskul. (2009)"Quick monitoring of pozzolanic reactivity of
384 waste ashes." *Waste Management*, 29(9), 1526-1531.

385 Tuan, N.V., G. Ye, K.V. Breugel, and O. Copuroglu. (2011) "Hydration and microstructure of
386 ultra high performance concrete incorporating rice husk ash." *Cement and Concrete Research*,
387 41(11), 1105-1111.

388 Wansom, S., S. Janjaturaphan, and S. Sinthupinyo. (2010) "Characterizing pozzolanic activity of
389 rice husk ash by impendence spectroscopy." *Cement and Concrete Research*, 40(12), 1714-1722.

390 Wansom, S., S. Janjaturaphan, and S. Sinthupinyo. (2009) "Pozzolanic Activity of Rice Husk
391 Ash: Comparison of Various Electrical Methods." *Journal of Metals, Materials and Minerals*,
392 19(2), 1-7.

393 Zheng, Y., Z. Pan, and R. Zhang. (2009) "Overview of biomass pretreatment for cellulosic
394 ethanol production." *International Journal of Agricultural and Biological Engineering*, 2(3), 51-
395 68.

396

397 **1. List of tables**

398 Table 1: ASTM C 150 Type I/II ordinary portland cement (OPC) Composition..... 19
399 Table 2: Oxide composition of selected ARA 20
400 Table 3: BET data for WSA and RSA under different burning conditions 21
401 Table 4: Effect of holding time on LOI and amorphous silica content 22

402

403 **2. List of figures**

404 Figure 1: Potassium (K) concentration for wheat straw 23
405 Figure 2: Ca (a) and (b) Mg concentration for wheat straw 23
406 Figure 3: Arrhenius Plot for wheat straw..... 24
407 Figure 4: Amorphous silica content of pretreated and untreated ARA 24
408 Figure 5: ARA amorphous silica vs ARA (WSA and RSA) oxide content..... 25
409 Figure 6: LOI of pretreated and untreated ARA..... 25
410 Figure 7: ARA LOI V vs ash K₂O, CaO and MgO content..... 25
411 Figure 8: Color of wheat straw ash, a) HCl80/24 pretreated and b) untreated 26
412 Figure 9: Particle size distribution of OPC and ARAs 26
413 Figure 10: Electrical conductivity change of HCl pretreated wheat straw ash..... 26
414 Figure 11: Electrical conductivity change wheat straw ash with different pretreatments 27
415 Figure 12: Heat flow rate of paste samples containing different wheat straw ash 27
416 Figure 13: Total heat of hydration of paste samples containing different wheat straw ash..... 28
417 Figure 14: Heat evolution rate of paste samples with and without rice straw ash..... 28
418 Figure 15: CH content of cement paste containing wheat straw ash 28
419 Figure 16: CH content of cement paste containing rice straw ash..... 29

420 Figure 17: Mortar cube compressive strength data..... 29

421 Figure 18: Relation between material characteristics and performance a) amorphous silica

422 content vs 28 days mortar cub strength, b) amorphous silica content vs CH content of paste after

423 90 days c) Surface area of ash vs CH content of paste after 90 days 30

424

425

426

427

428

429

Table 1: ASTM C 150 Type I/II ordinary portland cement (OPC) Composition

Chemical Composition (wt%)	
SiO ₂	21.85
Fe ₂ O ₃	3.4
Al ₂ O ₃	4.35
CaO	64.19
MgO	1.79
K ₂ O	0.52
Na ₂ O	0.17
SO ₃	2.77
LOI	0.89
Blaine Surface area= 362 m ² /kg	

430

431

432

433 **Table 2: Oxide composition of selected ARA**

Ash Type	SiO ₂	Al ₂ O ₃	Fe ₂ O ₃	CaO	MgO	K ₂ O	Na ₂ O
WSA-Cont-650/1	66.3	0.26	1.12	14.3	3.05	14.7	0.15
WSA-DW80-650/1	78.8	0.12	1.05	13.2	2.61	4.4	0.12
WSA-HCl80-650/1	86.5	0.28	1.13	9.73	0.78	1.54	0.1
WSA-HCl80-500/2	87.9	0.05	1.07	9.63	0.63	0.7	0.08
RSA-Cont-650/1	79.1	0.34	0.82	11.6	2.54	5.18	0.5
RSA-DW80-650/1	85.4	0.45	0.92	10.69	1.36	0.96	0.26
RSA-HCl80-650/1	88.2	0.47	0.74	9.48	0.56	0.31	0.17
RSA-HCl80-500/2	85.7	1.4	1.02	10.73	0.6	0.34	0.23

434

435

436

437

Table 3: BET data for WSA and RSA under different burning conditions

Ash type	BET surface area (m ² /g)
WSA-Cont-500/2	27.6
WSA-Cont-650/1	8.3
WSA-HCl80/24-500/2	168
WSA-HCl80/24-650/1	65
WSA-HCl80/24-700/1	39.7
RSA-Cont-500/2	16.9
RSA-Cont-650/1	9.6
RSA-HCl80/24-500/2	200
RSA-HCl80/24-650/1	134.5
RSA-DW80/24-650/1	58.94

438

439

440

441

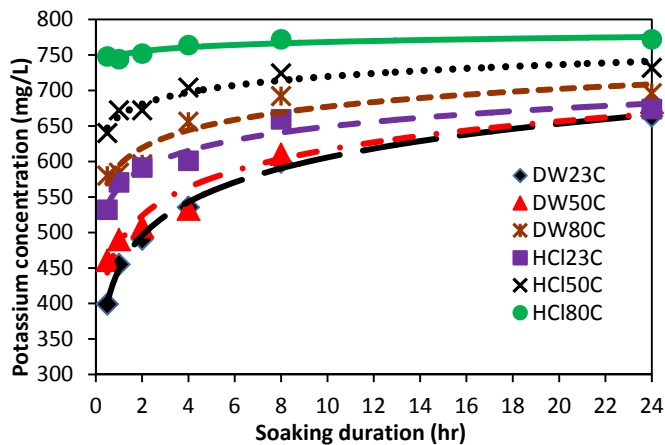
Table 4: Effect of holding time on LOI and amorphous silica content

WSA type	Amorphous Silica (%)	LOI (%)
HCl80/24-500/1	72.70	17.58
HCl80/24-500/2	88.65	2.76
HCl80/24-500/3	88.7	2.62
HCl80/24-650/1	89.14	1.18
HCl80/24-650/2	88.99	1.1

442

443

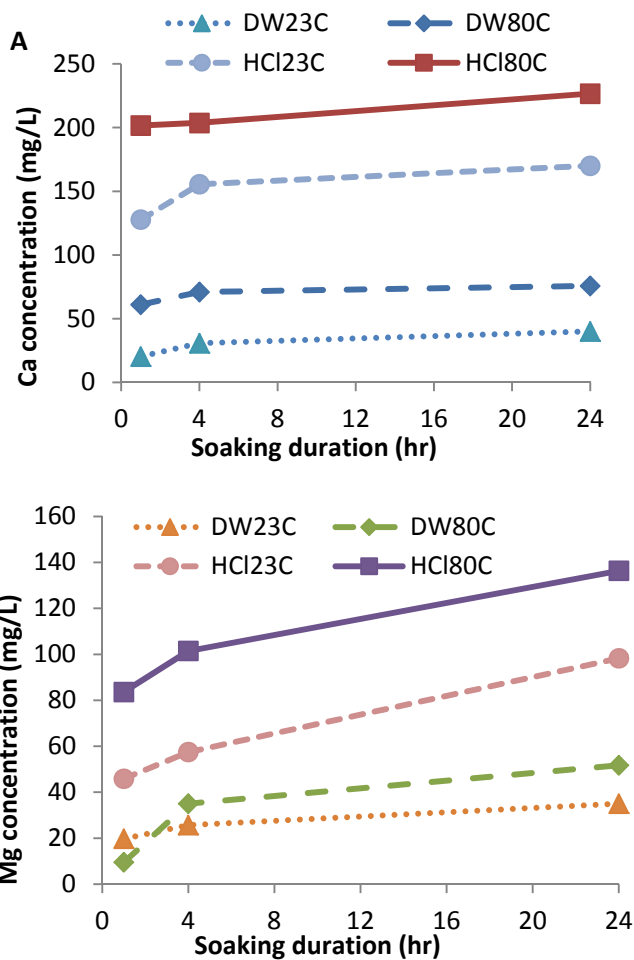
444



445

446

Figure 1: Potassium (K) concentration for wheat straw

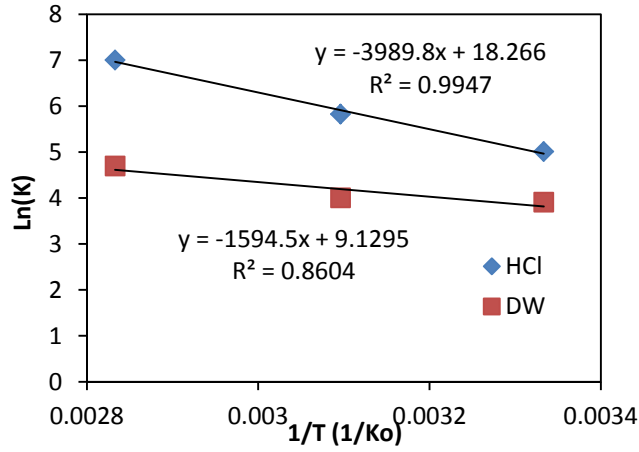


447

448

449

Figure 2: Ca (a) and (b) Mg concentration for wheat straw

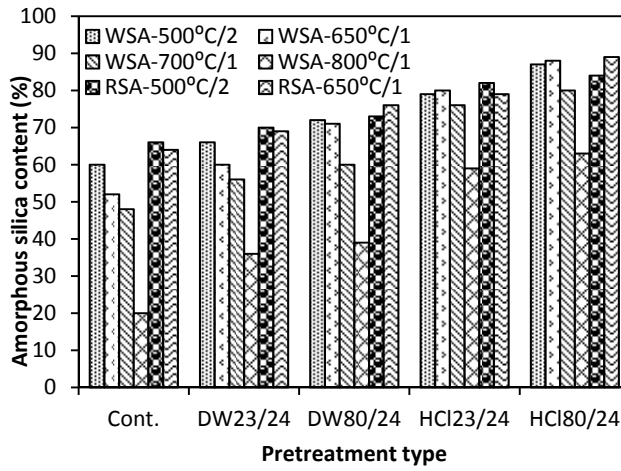


450

451

Figure 3: Arrhenius Plot for wheat straw

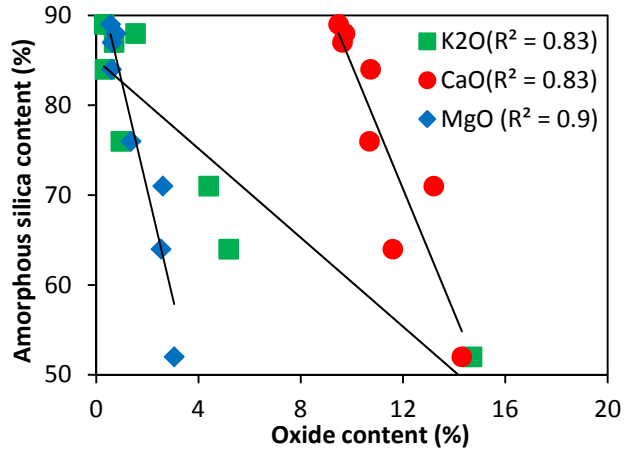
452



453

454

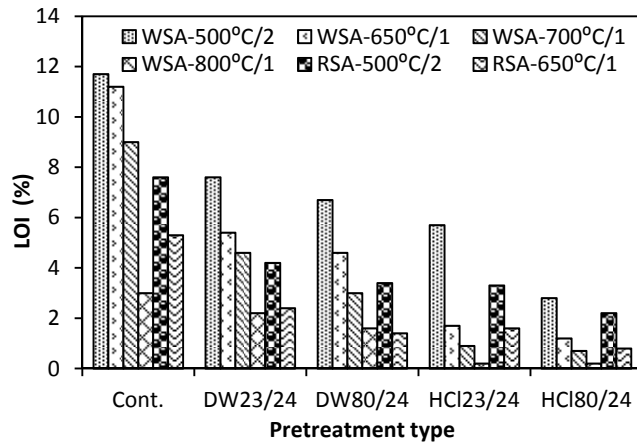
Figure 4: Amorphous silica content of pretreated and untreated ARA



455

456

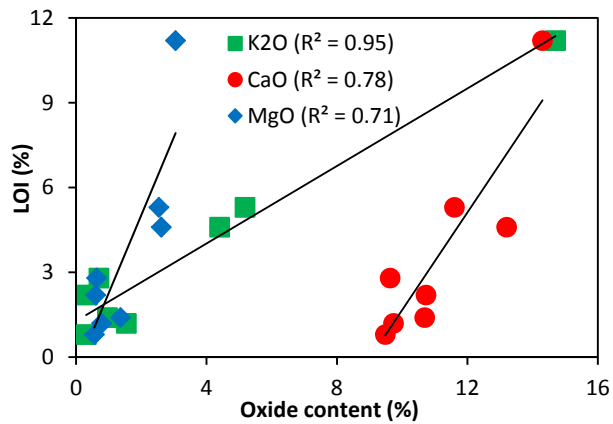
Figure 5: ARA amorphous silica vs ARA (WSA and RSA) oxide content



457

458

Figure 6: LOI of pretreated and untreated ARA

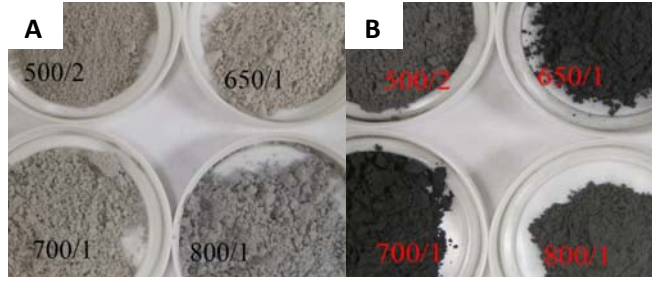


459

460

Figure 7: ARA LOI V vs ash K₂O, CaO and MgO content

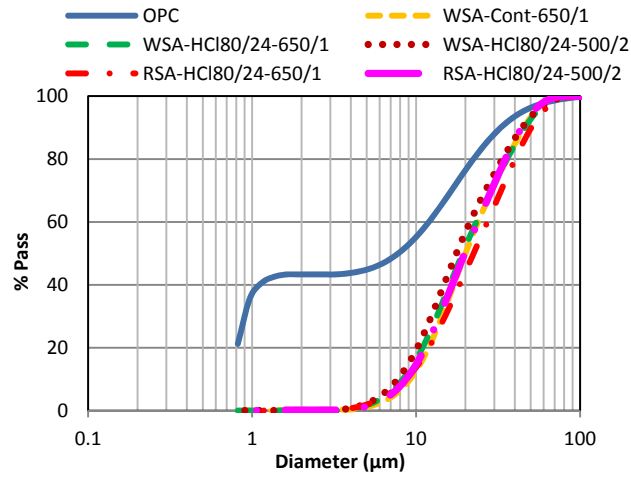
461



462

Figure 8: Color of wheat straw ash, a) HCl80/24 pretreated and b) untreated

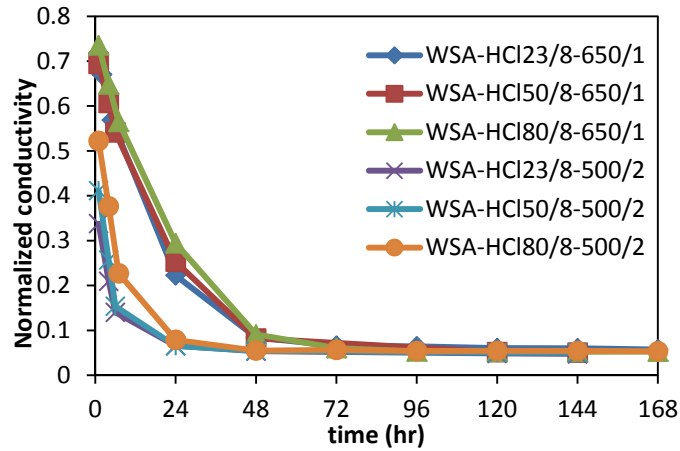
463



464

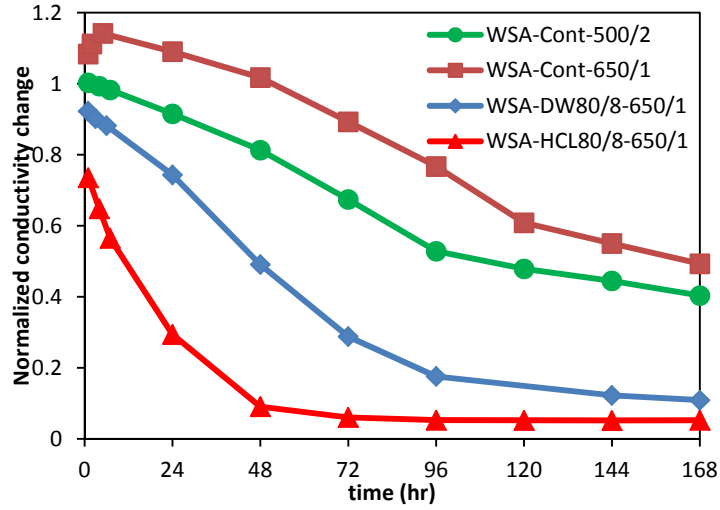
Figure 9: Particle size distribution of OPC and ARAs

465



466

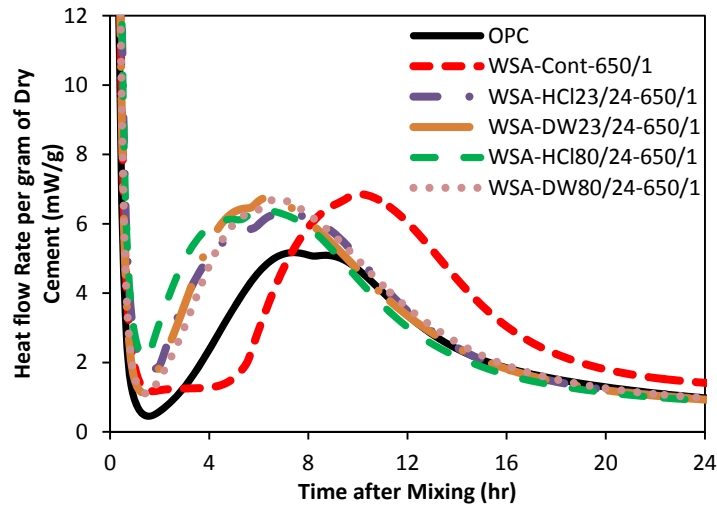
Figure 10: Electrical conductivity change of HCl pretreated wheat straw ash



467

468

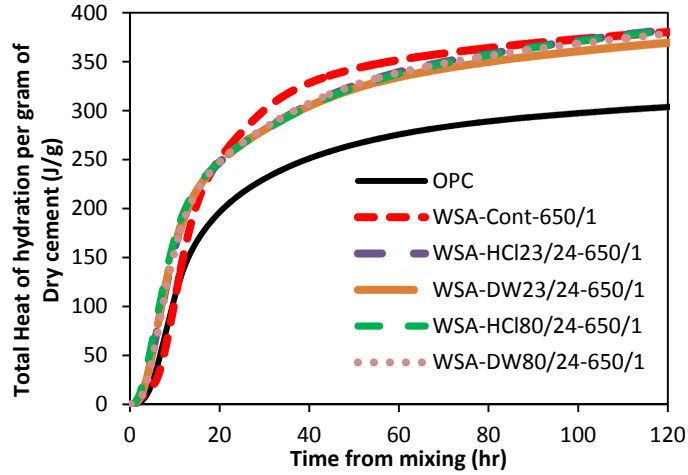
Figure 11: Electrical conductivity change wheat straw ash with different pretreatments



469

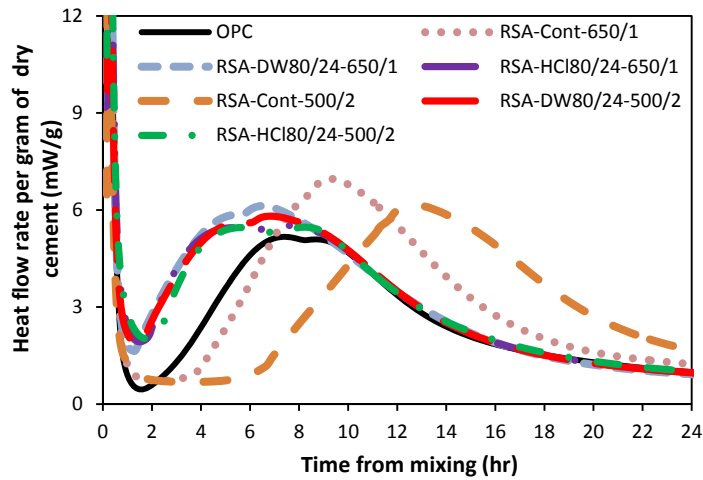
470

Figure 12: Heat flow rate of paste samples containing different wheat straw ash



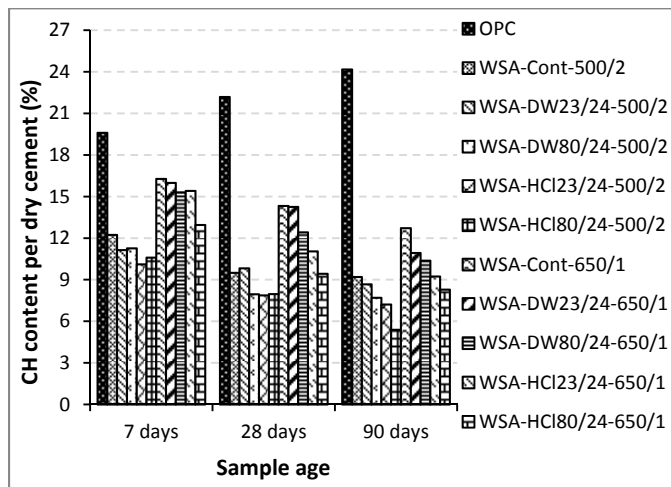
471

472 **Figure 13: Total heat of hydration of paste samples containing different wheat straw ash**



473

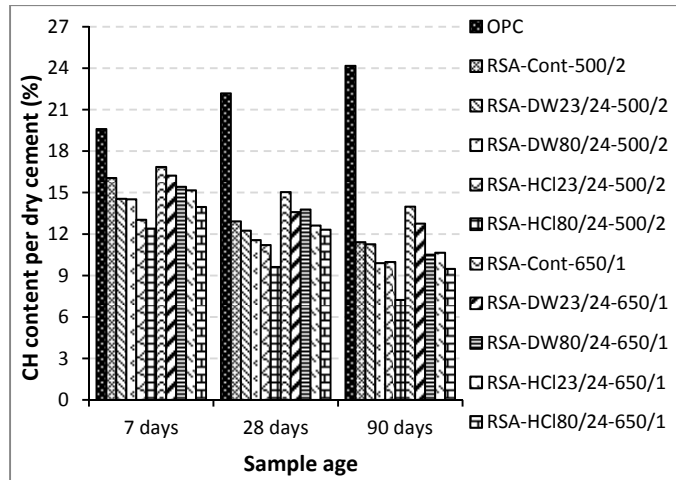
474 **Figure 14: Heat evolution rate of paste samples with and without rice straw ash**



475

476 **Figure 15: CH content of cement paste containing wheat straw ash**

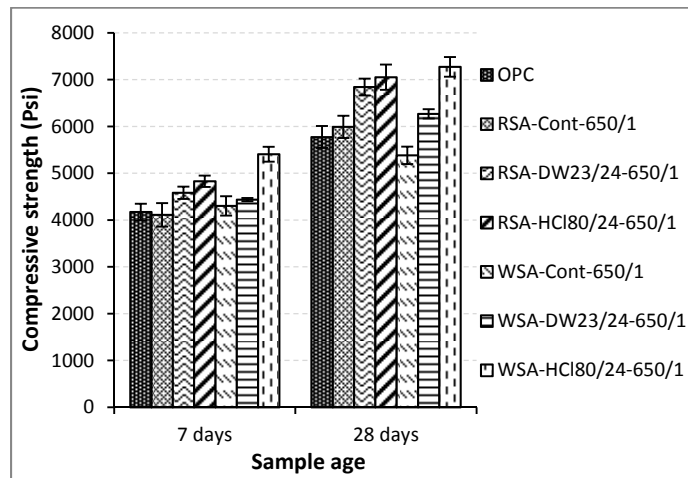
477



478

Figure 16: CH content of cement paste containing rice straw ash

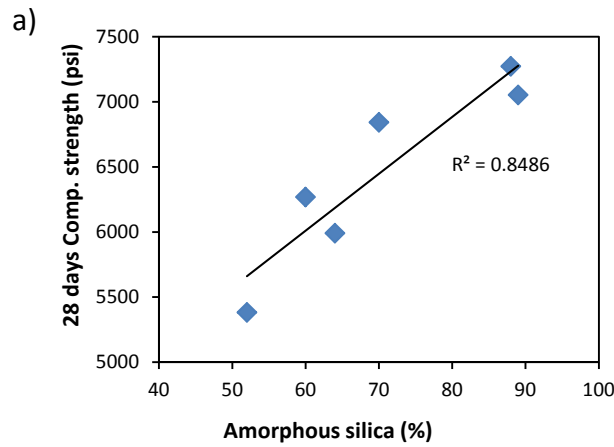
479

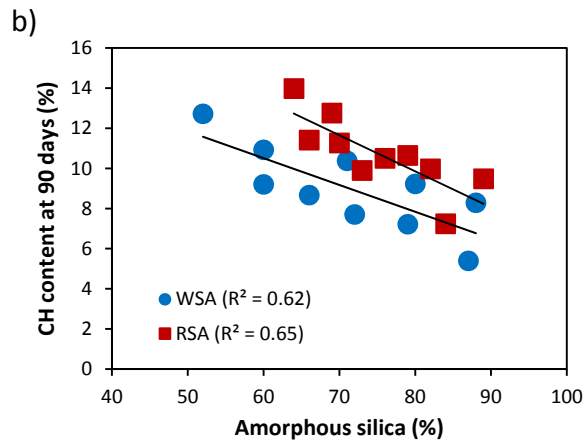


480

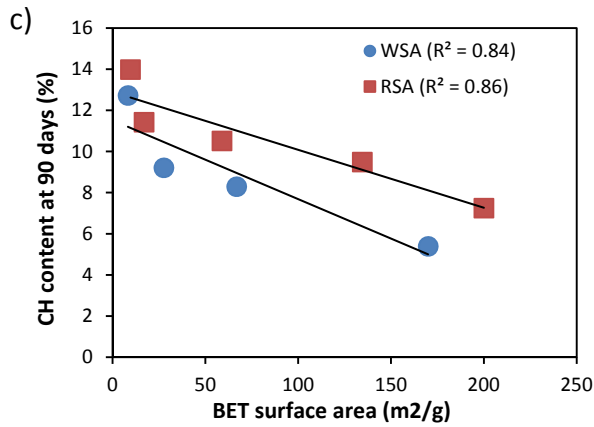
Figure 17: Mortar cube compressive strength data

481





482



483

484 **Figure 18: Relation between material characteristics and performance a) amorphous silica**

485 **content vs 28 days mortar cub strength, b) amorphous silica content vs CH content of paste**

486 **after 90 days c) Surface area of ash vs CH content of paste after 90 days**